

## Vortex dynamics in inhomogeneous superconducting films

S. A. Trugman\* and S. Doniach†

*Departments of Physics and Applied Physics, Stanford University, Stanford, California 94305  
and Groupe de Physique des Solides de l'Ecole Normale Supérieure, associé au Centre National  
de la Recherche Scientifique, Université Paris VII, 2 Place Jussieu, 75221 Paris-Cedex 05, France*

(Received 21 September 1981)

A vortex moving without dissipation in a superconducting film containing random inhomogeneities is shown to have a strictly periodic trajectory. By exploiting a new percolation analogy, the voltage noise power and the electrical resistivity due to a vortex are described at low frequencies in the zero-drag limit by the universal form  $P(\omega) \sim \omega^{p_2}$ , with  $p_2 \simeq 0.4$ . The introduction of dissipation into the vortex equations of motion modifies this form and causes resistivity to appear at zero frequency. Analogous effects should be observable in inhomogeneous superfluid  $^4\text{He}$  films.

### I. INTRODUCTION

In both superconductors and superfluid  $^4\text{He}$ , vortex excitations determine many of the equilibrium and dynamical properties. One of the most striking predictions is that of the onset of resistivity in thin films by means of a vortex unbinding phase transition.<sup>1-6</sup> Kosterlitz and Thouless observed that the static properties of this phase transition are identical to those of a two-dimensional Newtonian Coulomb gas.

In contrast to the static properties, the dynamics of vortices in a pure, frictionless superfluid or superconductor are distinctly different from those of Newtonian particles. The vortices drift in the local superfluid velocity.<sup>7-9</sup> The equations of vortex motion are first order in time in contrast to the second-order Newtonian case, and vortices move perpendicular to the energy gradient instead of accelerating along the gradient. It is not possible to distinguish between vortex and Newtonian dynamics on the basis of static measurements, since in a uniform sample both are consistent with the Boltzmann weight function ( $e^{-\beta U}$ ) for the probability of a given configuration. The consequences of vortex dynamics are apparent only in dynamical measurements such as the voltage noise-power spectrum of a superconducting film, or equivalently, by the fluctuation-dissipation theorem, the frequency dependent impedance.

Typically, the superconducting films are not homogeneous, having a thickness and composition that varies from point to point in space. As a result the general case involves a complicated simultane-

ous interaction of vortices with each other and with inhomogeneities. Two simplifying regimes are apparent: that where vortex-substrate interactions are negligible compared with vortex-vortex interactions, and the opposite extreme. The first regime is discussed in Sec. II; an exact result due to Helmholtz shows that vortex dynamics lead to no voltage fluctuations at all for a homogeneous film. The second regime, that of a single vortex interacting with an inhomogeneous substrate, is the principal subject of this paper. Some remarks on the general case are made in Sec. V and Appendix C.

It is not expected that the ideal vortex dynamics described above apply exactly in any realizable systems. *Superfluid* vortices experience drag due to interaction with quasiparticle excitations (normal fluid). If the interactions causing dissipation are weak, vortices travel generally with the local superflow, but with a small component down the energy gradient. If the interactions are quite strong, the motion becomes identical to that of Newtonian particles in a viscous medium: Vortices diffuse down the energy gradient. Bardeen and Stephen<sup>10</sup> have argued that this picture does not apply to superconductors, and that ideal vortex dynamics are in principle unobservable due to the positive ionic background. Nozières and Vinen<sup>11</sup> have criticized this analysis, showing that the Magnus force that leads to ideal vortex dynamics in helium is unaltered in superconductors. It is this latter point of view that we adopt in this work. This work focuses on the no-drag and low-drag regimes where the unique vortex dynamics leaves its mark.

We show that for a randomly disordered film

without dissipation, a vortex does not wander at random, but rather forms a closed periodic orbit. Because of this "classical vortex confinement," an infinite film shows no resistivity at zero frequency. By exploiting a new mapping to the percolation problem, the probability of large orbits and the detailed behavior of a vortex on such an orbit can be calculated. This results in a voltage noise-power spectrum or resistivity that scales like a power of the frequency, with a universal exponent which we show is given in terms of known percolation critical indices.

The addition of a small amount of drag to the equations of motion results in a dc resistivity; the power law crosses over to a constant at small frequencies. The zero-frequency limit of this theory is in qualitative agreement with dc data taken on granular NbN films. Systematic finite-frequency data of a nature described in Sec. V would provide a far better test, but so far as we know, have not yet been measured.

It would appear that the low-drag vortex dynamics described in this work would be unobservable in nongranular superconducting films, which are in the high-drag limit. We believe, however, that vortices in some *granular* films may move through the insulating regions with very low effective drag. In Appendix D we give a quantitative estimate of the drag that would be expected in a granular film. This estimate is based on the experimentally observed low-drag vortex dynamics in long tunnel junctions.

A second system in which low-drag vortex dynamics should be observable is superfluid  $^4\text{He}$  films. In superfluid helium films, a superflow can be applied by an oscillating substrate, as was done by Bishop and Reppy,<sup>12</sup> or by applying a temperature gradient (third sound). Frequency-dependent dissipation due to vortices can be measured as a function of frequency, as in superconducting impedance measurements. The discussion that follows will, however, be geared mainly toward superconductors.

This paper is organized as follows: Section I is an introduction. In Sec. II we derive the equations of vortex dynamics and discuss energetic and equilibrium issues. Section III is concerned with the percolation analogy and noise-power scaling under pure vortex dynamics. In Sec. IV we add drag to the equations of motion and derive the resultant noise-power spectrum. Section V is concerned with experimental considerations and a discussion of the domains in which the theory applies. A summary and conclusions are found in Sec. VI. There are

four appendixes: Appendix A treats some details of the finite-drag case, Appendix B calculates the constants required to express the voltage noise power in volts, and Appendix C discusses the modifications that result either when the vortices form a lattice or when they occur in a sample of finite size. Appendix D discusses the possibility that vortices may move with low drag in some granular films.

## II. VORTEX EQUATIONS OF MOTION

### A. Ideal vortex dynamics

We start from the equations of vortex motion. The derivation is a generalization of that given by Ambegaokar, Halperin, Nelson, and Siggia,<sup>13</sup> hereafter referred to as AHNS. We consider a thin-film superconductor that varies in composition and/or thickness as a function of position. We also write the equations of motion in terms of energy rather than supercurrent velocity, which will be important in the following development.

The supercurrent is given by

$$\vec{j}' = -2e |\psi|^2 \vec{v}'_s, \quad (2.1)$$

where  $\psi = |\psi| e^{i\phi}$  is the order parameter and  $|\psi(\vec{r})|^2$  is the number density of Cooper pairs at point  $\vec{r}$ . The velocity of the supercurrent is

$$\vec{v}'_s = \frac{\hbar \vec{\nabla} \phi}{2m} - \frac{e \vec{A}}{mc}. \quad (2.2)$$

We will neglect the diamagnetic term (proportional to the gauge field  $\vec{A}$ ) in a vortex velocity field. In a thin film, it is negligible compared with the  $\vec{\nabla} \phi$  term out to the large distance from the core  $\Lambda = 2\lambda^2 / \langle d \rangle$ , where  $\lambda$  is the bulk London screening length and  $\langle d \rangle$  is the average film thickness.

The first step is to derive the velocity of the supercurrent for a given vortex configuration. Let  $\vec{v}_s$  be the transverse part ( $x$  and  $y$  components) of the velocity field averaged over the thickness  $d(x, y)$ . Define  $\vec{J}$  as the transverse part of the supercurrent, *integrated* over the thickness of the film,

$$\vec{v}_s(x, y) = d(x, y)^{-1} \int_0^{d(x, y)} dz \vec{v}'_s(x, y, z), \quad (2.3)$$

$$\vec{J}(x, y) = \int_0^{d(x, y)} dz \vec{j}'(x, y, z).$$

(The  $z$  components of  $\vec{v}_s$  and  $\vec{J}$  are then set equal to zero.) We assume that the vortex lines are in the  $\hat{z}$  direction and that the film thickness changes slowly ( $|\vec{\nabla} d| \ll 1$ ) so that they remain nearly vertical as they move.  $\vec{J}$  and  $\vec{v}_s$  satisfy

$$\begin{aligned}\vec{\nabla} \cdot \vec{J} &= 0, \\ \vec{\nabla} \times \vec{v}_s &= \frac{\pi \hbar}{m} n(\vec{r}) \hat{z}, \\ \vec{J} &= -2e |\psi|^2 d \vec{v}_s,\end{aligned}\quad (2.4)$$

where all derivatives are in the  $x$ - $y$  plane only. The variables  $|\psi|^2$ ,  $d$ , and  $n$  are functions of  $x$  and  $y$ . The position-dependent superfluid density  $|\psi^2(\vec{r})|$  can be obtained by solving a Ginzburg-Landau equation for the inhomogeneous sample. The norm  $|\psi^2(\vec{r})|$  does not depend on the number and location of vortices (except at the vortex cores, which are assumed small). The variable  $n$  is the density of vortices per unit area

$$n(\vec{r}) = \sum_j n_j \Delta(\vec{r} - \vec{r}_j)$$

with  $n_j (= \pm 1)$  the sign of vortex  $j$ , and  $\Delta$  a function of unit weight and the width of a vortex core. In the drag-free limit, a vortex drifts in the local superfluid velocity at its core

$$\dot{\vec{r}}_j = \vec{v}_s(\vec{r}_j). \quad (2.5)$$

Equations (2.4) and (2.5) together determine the motion of a system of vortices in an inhomogeneous film specified by  $|\psi^2(\vec{r})| d(r)$ .

The qualitative features of the solutions of Eq. (2.4) are made more apparent by noting that they are identical to those of two-dimensional electrostatics if one rotates  $\vec{J}$  and  $\vec{v}_s$  by  $90^\circ$ . Defining

$$\begin{aligned}\vec{D} &\equiv -\hat{z} \times \vec{v}_s, \\ \vec{E} &\equiv \frac{1}{2e |\psi_0|^2 d_0} \hat{z} \times \vec{J},\end{aligned}\quad (2.6)$$

we obtain

$$\begin{aligned}\vec{\nabla} \times \vec{E} &= 0, \\ \vec{\nabla} \cdot \vec{D} &= 2\pi\rho, \\ \vec{D} &= \epsilon \vec{E},\end{aligned}\quad (2.7)$$

with  $\rho = (\hbar/2m)n(\vec{r})$  and  $\epsilon(\vec{r}) = |\psi_0|^2 d_0 / [|\psi^2(\vec{r})| d(\vec{r})]$ . The term  $|\psi_0|^2 d_0$  is  $|\psi^2(\vec{r})| d(\vec{r})$  evaluated at an arbitrary point  $\vec{r}_0$ . The problem of determining the supercurrent is thus isomorphic to that of solving for the electric field of charges in a position-dependent dielectric medium.<sup>14(a)</sup> In the context of this analogy, vortices will sometimes be referred to as "charges" in the discussion below.

The kinetic energy of the electrons is

$$U_{\text{kin}} = \int d^2\vec{r} m |\psi^2(\vec{r})| \vec{v}_s^2(\vec{r}) d(\vec{r}). \quad (2.8)$$

Substituting for  $\vec{v}_s$ , this can be written

$$U_{\text{kin}} = 4\pi m |\psi_0|^2 d_0 \left[ \frac{1}{4\pi} \int d^2\vec{r} \vec{D} \cdot \vec{E} \right]. \quad (2.9)$$

The kinetic energy of the supercurrents is thus proportional to the Coulomb energy of the electrostatics problem (the electrostatic energy  $U_{\text{Coul}}$  is the term in parentheses).

Noting that the electric field acting on a charge is given by  $q\vec{E} = -\vec{\nabla} U_{\text{Coul}}$ , we can solve for the local superfluid velocity ( $\hat{z} \times \vec{D}$ ) at the location of vortex  $j$  in terms of the kinetic energy gradient

$$\vec{v}_s(\vec{r}_j) = \frac{-n_j}{2\pi\hbar |\psi|^2 d} \hat{z} \times \vec{\nabla}_j U_{\text{kin}}. \quad (2.10)$$

The gradient is with respect to  $\vec{r}_j$ .

The kinetic energy of the electrons (or equivalently the electrostatic energy of the charges) can be calculated exactly only if  $\epsilon(\vec{r})$  has high symmetry. In the general case it must be obtained numerically. One can, however, note qualitatively that a charge has a lower energy in a neighborhood where the dielectric constant is large; correspondingly, a vortex has a lower energy in a region where the film is thin and  $|\psi|^2$  is small.

It is important that the energy used in Eq. (2.10) be calculated with the correct vortex core size  $\xi_v$ , and not in the limit of point charges ( $\xi_v \rightarrow 0$ ). If the dielectric constant is space dependent,  $\vec{\nabla} U$  will diverge for  $\xi_v \rightarrow 0$ , resulting in infinite vortex velocities from Eq. (2.10). No such problem arises for a constant  $\epsilon$ , however.

## B. Effect of dissipative and conservative forces

Equation (2.5) must be generalized in the case where forces other than the Lorentz force act on a vortex. The Lorentz force is given by<sup>11</sup>

$$\vec{F}_L = 2\pi\hbar |\psi|^2 d n_j \hat{z} \times \left[ \frac{d\vec{r}}{dt} - \vec{v}_s(\vec{r}) \right]. \quad (2.11)$$

Since a vortex core is massless, or nearly so, it must move with a velocity such that the total force on it is zero. The condition that the Lorentz force vanishes is equivalent to Eq. (2.5) for the velocity.

In general, there is an additional conservative force  $\vec{f}' = -\vec{\nabla} U'$  acting on a vortex. The origin of this force is the work necessary to make a vortex core longer, or to move it into a region where  $|\psi|^2$  is larger. There are also drag forces on a vortex core due to interactions with the ionic lattice of the

superconductor and with quasiparticle excitations, assumed at rest in the lattice frame. The drag force is assumed to be of the form<sup>14(b)</sup>

$$\vec{F}_D = |\psi|^2 d \left[ -b_1 \frac{d\vec{r}}{dt} - b_2 n_j \hat{z} \times \frac{d\vec{r}}{dt} \right]. \quad (2.12)$$

One must also include a Langevin noise term, representing fluctuations induced by quasiparticles, whenever there is a dissipative term ( $b_1 \neq 0$ ), so that the system will come to thermal equilibrium.

The velocity of a vortex is that for which the net force on it vanishes, where the net force is the sum of  $\vec{F}_L$ ,  $\vec{f}'$ ,  $\vec{F}_D$ , and the Langevin force. The velocity is given by

$$\dot{\vec{r}}_j = \frac{1}{|\psi|^2 d} (-\alpha n_j \hat{z} \times \vec{\nabla} U - \Gamma \vec{\nabla} U) + \vec{\eta}_j(t) \quad (2.13)$$

with

$$\alpha = \frac{2\pi\hbar - b_2}{b_1^2 + (2\pi\hbar - b_2)^2}, \quad (2.14)$$

$$\Gamma = \frac{b_1}{b_1^2 + (2\pi\hbar - b_2)^2}.$$

Here,  $\vec{\eta}_j(t)$  is the Langevin Gaussian white-noise term and  $U$  is the total energy,  $U = U' + U_{\text{kin}}$ . In the absence of drag ( $b_1 = \eta = 0$ ), the coefficient  $\Gamma$  of Eq. (2.13) vanishes. Equation (2.13) then states that a vortex moves perpendicular to the energy gradient, conserving the total energy of the system.

The fact that  $|\psi|^2 d$  is explicitly position dependent leads to a different result from that obtained in the uniform case as the system comes to thermal equilibrium. The Langevin noise should be chosen to satisfy

$$\langle \eta_i^\alpha(t) \eta_j^\beta(t') \rangle = 2D \delta_{ij} \delta_{\alpha\beta} \delta(t - t'). \quad (2.15)$$

$D$  is the local diffusion constant and must be explicitly position dependent

$$D(\vec{r}) = \frac{k_B T \Gamma}{|\psi(\vec{r})|^2 d(\vec{r})}. \quad (2.16)$$

This will allow the system to come to equilibrium with a probability  $P$  of finding a vortex in a region of area  $dx dy$  given by

$$P(\vec{r}) = ce^{-\beta U(\vec{r})} dx dy / \epsilon(\vec{r}). \quad (2.17)$$

Note that the correct measure is not simply  $dx dy$ , but rather  $dx dy / \epsilon(\vec{r})$ . (This reduces to  $dx dy dz$  if  $|\psi|^2$  is constant.) With the choice (2.16) for  $D$ , the density (2.17) is stationary

$$\frac{\partial P(\vec{r})}{\partial t} = -\vec{\nabla} \cdot \vec{J}_{\text{vortex}}(\vec{r}) = 0. \quad (2.18)$$

It is not possible to choose a different definition of  $D(\vec{r})$  such that the distribution with the ordinary measure

$$P'(\vec{r}) = ce^{-\beta U(\vec{r})} dx dy$$

is stationary. The reason, on one level, is that in the drag-free case Liouville's theorem (that the volume of a region in phase space is constant as it time evolves) is true only if the measure used is  $dx dy / \epsilon(\vec{r})$ .

### C. Experimental consequences; uniform substrates

One can experimentally test the equations of motion (2.13) by measuring the voltage induced across the length  $L_2$  of a thin film of width  $L_1$  (see Fig. 1). By the fluctuation-dissipation theorem, one could equivalently measure the frequency-dependent impedance. By the standard phase-slip argument,<sup>15</sup> the voltage is given by

$$V(t) = \frac{\pi\hbar}{eL_1} \sum_j n_j \dot{y}_j(t), \quad (2.19)$$

where  $\dot{y}_j$  is the component of the velocity of vortex  $j$  perpendicular to the length direction. It would be particularly interesting to study a system in which the  $\alpha$  term dominates the  $\Gamma$  term in Eq. (2.13), since that is the situation in which the unique vortex dynamics appear.

The situation in which a system of vortices moves without drag on a uniform substrate can be handled directly. In this case the equations of motion become

$$\dot{\vec{r}}_j = -\frac{\hbar}{2m} n_j \hat{z} \times \vec{\nabla}_j (U/q^2), \quad (2.20)$$

where

$$(U/q^2) = -\sum_{i < j} n_i n_j \ln(|\vec{r}_i - \vec{r}_j|/b). \quad (2.21)$$

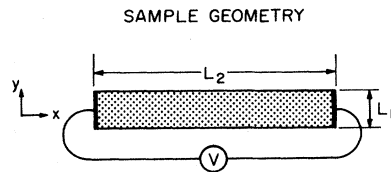


FIG. 1. Diagram of the voltage noise-power measurement apparatus.

AHNS point out that an isolated  $\pm$  vortex pair moving according to Eq. (2.20) will result in no measured voltage since its dipole moment remains constant. This observation does not apply to a system of more than two vortices. Helmholtz has, however, proven a theorem that gives the corresponding result for an arbitrary system of vortices.<sup>7</sup>

$$\sum_j n_j \vec{v}_j = 0. \quad (2.22)$$

This result applies whether or not  $\Lambda \gg R$ . Equation (2.19) implies that there is no voltage in the zero-drag limit for vortices on a uniform substrate. Taking a specific example, when two vortex pairs interact, the dipole moment of each pair changes, but in such a manner that the sum of the dipole moments is time independent.

Neither Eq. (2.22) nor the above zero-voltage result holds if vortices interact with the boundaries (through image vortices) of a finite system. A boundary is just a special case of an inhomogeneity, so that in general we must look at an inhomogeneous substrate to see vortex dynamics in the type of experiment described above. The simplest system with nonvanishing effects is that of a single vortex interacting with an inhomogeneous substrate, or equivalently a dilute one-component plasma injected by a magnetic field in which vortex-vortex interactions can be neglected compared with vortex-substrate interactions. This system will be analyzed in the following section.

### III. IDEAL SINGLE VORTEX MOTION IN AN INHOMOGENEOUS FILM

#### A. Model potential

In this section we consider a single vortex moving without drag in an inhomogeneous film according to

$$\dot{\vec{r}}_j = \frac{-n_j}{2\pi\hbar |\psi^2(\vec{r})| d(\vec{r})} \hat{z} \times \vec{\nabla} U(\vec{r}). \quad (3.1)$$

$U(\vec{r})$  is the total energy, which is the sum of the kinetic energy of the superconducting electrons and the energy due to any conservative forces acting on the vortex. For a randomly disordered substrate, consisting for example of independent grains,  $U(\vec{r})$  will be a rapidly varying function of position. We will assume that  $U$  can be adequately represented by white noise with a high-frequency cutoff. In particular, we will assume a model in which an independent random number  $U_j$  is assigned to each vertex

of a triangular lattice. The potential  $U(\vec{r})$  is given by  $U_j$  if  $\vec{r}$  is the position of vertex  $j$ . The potential in the interior of a triangle is given by the plane containing the vertices of the triangle (see Fig. 2).  $U(\vec{r})$  plotted above the  $x$ - $y$  plane will then be a patchwork of connected triangles of random slopes. The vertices are chosen to be a distance  $b$  apart, where  $b$  is the correlation length of the potential  $U$ . The results we obtain apply to a class of potentials much broader than that of our model, as they are obtained from the critical properties of an entire universality class. In particular, the actual potential  $U$  is better modeled if the random variables  $U_j$  are not completely independent. If the correlations are sufficiently weak, the corresponding percolation problem belongs to the same universality class as the uncorrelated percolation problem, and the results we obtain will apply. This will become clearer later in the section.

#### B. Connection with the percolation problem

In this section we show how the vortex trajectories are related to the percolation problem. To be concrete, we assume that the potential energies  $U_j$  of the model potential  $U$  are independent random variables distributed uniformly between  $-V/2$  and  $+V/2$ . According to Eq. (3.1), each trajectory will conserve energy. Consider a trajectory of energy  $E$ , and color all vertices of the lattice that have an energy less than  $E$  black. Each trajectory of energy  $E$  will be a closed curve that forms the perimeter of a connected cluster of black vertices. (See Fig. 3.) For a trajectory of near-minimum energy, the probability  $p$  of a given vertex being black will be small, and the connected black clusters will with high probability have only one or two vertices. The vortex trajectories will then be small closed curves.

MODEL POTENTIAL  $U(x,y)$

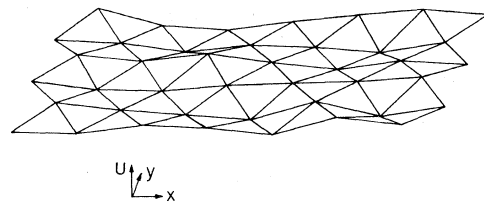


FIG. 2. Perspective drawing of the random model potential  $U(x,y)$ .

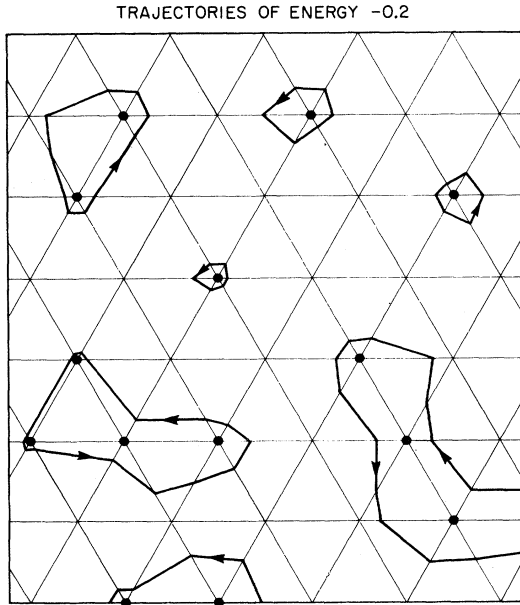


FIG. 3. Trajectories of (—) vortices in the presence of a randomly generated potential  $U$ , where  $-0.5 \leq U(x,y) \leq 0.5$ . (+) vortices move in the opposite sense. All vertices of energy less than  $-0.2$  are colored black. Vortex trajectories of energy  $-0.2$  circle connected clusters of black vertices.

As  $E$  increases, the average size of the connected clusters will grow. At exactly the median energy<sup>16</sup> (here  $E=0$ ), the black vertices will begin to percolate, and arbitrarily large clusters appear. This situation is illustrated in Fig. 4.

As  $E$  increases above zero, the trajectories get smaller, as they must, since the problem is symmetric in  $E \leftrightarrow -E$ . What occurs here is that with high probability the vortices are circling inside holes in the infinite percolating cluster of black vertices. In the language of topographic maps, the low-energy trajectories circle lakes, the high-energy trajectories circle mountaintops; those of near-median energy become quite large.

To calculate the average voltage noise-power spectrum of a vortex we need two components: the probability with which different trajectory lengths  $L$  occur, and the noise power due to a vortex on a trajectory of a particular  $L$ . The former calculation is done in Sec. IV. The noise power of a vortex on a given perimeter of length  $L$  is calculated below. The result is found in Eq. (3.19); it is expressed in terms of a new universal exponent  $p_1$ .

Consider a vortex circulating at constant speed  $v$  about a large connected cluster of black vertices, on a path of total perimeter  $L$  (we will discuss noncon-

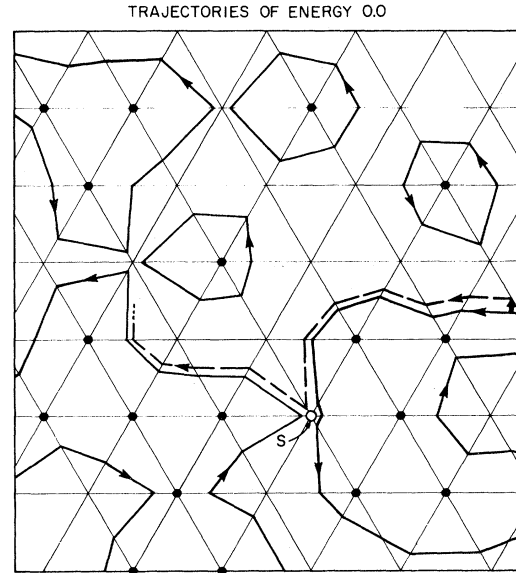


FIG. 4. Solid lines are (—) vortex trajectories of energy 0.0 in the presence of the same potential used in Fig. 3. The black dots here denote vertices of energy less than zero. These vertices are at the percolation threshold, so that some of the trajectories are arbitrarily large. The dashed line represents a portion of the trajectory of a vortex that was perturbed by Langevin noise (arrow, right center). It follows its old trajectory closely until it encounters a saddle-point vertex ( $S$ ).

stant speeds later in this section). Parametrize the vortex position  $\vec{r}$  by the arc length  $l$  between  $\vec{r}$  and a designated starting point  $\vec{r}_0$ . Since the motion is periodic, the  $y$  coordinate will be given by the Fourier series

$$y(l) = \sum_k e^{ikl} a_k, \quad (3.2)$$

$$a_k = L^{-1} \int_0^L dl y(l) e^{-ikl}, \quad (3.3)$$

where  $k$  assumes the values  $nk_0$  for all integers  $n$  with  $k_0 = 2\pi/L$ .

To derive the voltage noise-power spectrum we require the correlation functions  $\langle a_k a_{-k} \rangle$  for  $k = nk_0$ . The relevant relation, with the use of Eqs. (2.19) and (3.2), is

$$\langle V^2(t) \rangle = \left[ \frac{\pi \hbar v}{e L_1} \right]^2 \sum_k k^2 \langle a_k a_{-k} \rangle. \quad (3.4)$$

The angular brackets imply an average over all orbits of length  $L$ . Defining the voltage noise-power spectrum  $P(\omega)$  to satisfy

$$\langle V^2(t) \rangle = \int d\omega P(\omega), \quad (3.5)$$

$P(\omega)$  for a vortex on a trajectory of length  $L$  is given by

$$P(\omega) = \left[ \frac{\pi \hbar}{eL_1} \right]^2 \sum_n \delta(\omega - n\omega_0) \omega^2 \langle a_{\omega/v} a_{-\omega/v} \rangle, \tag{3.6}$$

where  $\omega_0 = vk_0$  and the sum is over the integers. Alternatively, Eqs. (3.4)–(3.6) can be taken as statements about the real part of the electrical impedance  $Z$  by using the Nyquist relation

$$\text{Re}[Z(\omega)] = \frac{\pi}{k_B T} P(\omega). \tag{3.7}$$

Further analysis is required to determine the precise form of  $P(\omega)$ . It is clear at this stage, however, that because the trajectories are periodic, a vortex on an orbit of length  $L$  puts out no noise power at frequencies smaller than  $\omega_0 = 2\pi v/L$ . Low-frequency noise power comes only from large orbits. There is no zero-frequency noise power, or equivalently there is no dc resistivity in the absence of drag, because any orbit is finite with probability one.

We now investigate the form of  $f(k) \equiv \langle a_k a_{-k} \rangle$  for vortices on large orbits. One of the central ideas of critical phenomena is that as the correlation length diverges, the typical configurations become scale invariant. In particular, a section of the perimeter of a large cluster is self-similar down to a scale of the order of the lattice spacing  $b$ . This self-similarity is the defining property of a fractal.<sup>17</sup> The only scale-invariant form that  $f(k)$  can assume is

$$f(k) \equiv \langle a_k a_{-k} \rangle = c_1(L) k^{-p_1}. \tag{3.8}$$

The exponent  $p_1$  has not previously been discussed for the percolation problem. We relate it to the usual critical indices for the percolation problem by calculating the relationship between the diameter of a cluster and its perimeter. The square of the difference in the  $y$  coordinates of two points on the perimeter of a cluster is

$$\begin{aligned} \langle [y(l_2) - y(l_1)]^2 \rangle &= \sum_{k,q} (e^{ikl_2} - e^{ikl_1}) \\ &\quad \times (e^{iq l_2} - e^{iq l_1}) \langle a_k a_q \rangle. \end{aligned} \tag{3.9}$$

Using Eq. (3.8) and approximating the sums by integrals, Eq. (3.9) yields

$$\begin{aligned} \langle [\Delta y(l)]^2 \rangle &= l^{p_1-1} \left[ 4b' \pi^{-1} \int_0^{\pi l/b} du \sin^2(u/2) u^{-p_1} \right], \end{aligned} \tag{3.10}$$

where  $l = l_2 - l_1$  and  $c_1(L) = b'/L$ . For  $p_1 > 1$  and  $l/b \gg 1$ , the bracketed term on the right-hand side of the above equation is simply a constant. Then,

$$\langle [\Delta y(l)]^2 \rangle \sim l^{p_1-1}. \tag{3.11}$$

The result is that a large connected cluster of perimeter  $L$  will have a rms width of order

$$\xi \equiv \langle [\Delta y(L/2)]^2 \rangle^{1/2} \sim L^{(p_1-1)/2}. \tag{3.12}$$

The connection between  $p_1$  and the percolation-critical indices can now be made since the percolation critical index  $\nu$  is defined by

$$\xi(p) \sim |p - p_c|^{-\nu}, \tag{3.13}$$

where  $p_c$  is the smallest occupation probability for which the black vertices form an infinite connected cluster. The critical behavior is dominated by clusters containing  $\bar{s}$  sites where

$$\bar{s} \sim |p - p_c|^{-1/\sigma}. \tag{3.14}$$

Near the critical point, the total perimeter is proportional to the number of sites in the cluster (the clusters are said to be “ramified”<sup>18</sup>), so  $\sigma$  also describes the diverging perimeter

$$L \sim |p - p_c|^{-1/\sigma}. \tag{3.15}$$

Using Eqs. (3.13) and (3.15) we find that  $\xi \sim L^{\sigma\nu}$ . Comparing with Eq. (3.12), we now have the desired equation for the Fourier space exponent

$$p_1 = 2\sigma\nu + 1. \tag{3.16}$$

Numerical estimates compiled by Stauffer<sup>19</sup> of the percolation critical indices are that  $\sigma \simeq 0.39$  and  $\nu \simeq 1.3$ , which result in  $p_1 \simeq 2.0$ .

If desired, relation (3.16) can be expressed in terms of the Hausdorff-Besicovitch dimension  $D_H$  of a fractal.<sup>17</sup>  $D_H$  can generally be obtained heuristically using the formula  $L = \xi^{D_H}$  so that we have now obtained a connection between the fractal dimensionality  $D_H$  and the percolation critical indices

$$D_H = (\sigma\nu)^{-1}. \tag{3.17}$$

Relation (3.17) was previously derived by Stanley.<sup>20</sup> Using Eq. (3.17), we can rewrite Eq. (3.16) as

$$p_1 = 2/D_H + 1, \tag{3.18}$$

thus obtaining a relation between the fractal dimensionality and the autocorrelation function of a trajectory following the perimeter.

Equation (3.6) yields the voltage noise-power spectrum of a vortex traveling on an orbit of perimeter  $L'$  with  $p_1$  given by (3.16),

$$P(\omega) = c_1 \left[ \frac{\pi \hbar v}{e L_1} \right]^2 \sum_{n=-N'}^{N'} \delta(\omega - n \omega_0) (\omega/v)^{2-p_1}. \quad (3.19)$$

We have introduced a cutoff  $N' \simeq L/b$ , which is intended to represent approximately the fact that the scaling form of Eq. (3.8) breaks down when  $k$  becomes as large as an inverse lattice spacing. At smaller distances than this, the trajectories are smooth and the Fourier amplitudes drop rapidly to zero.

Equation (3.19) was derived under the assumption that the speed  $v$  of a vortex is constant. In fact, Eq. (3.1) states that the speed is proportional to the magnitude of the local energy gradient, which can assume any value between zero and  $2V/(3^{1/2}b)$ . The average speed  $\bar{v}$  with which a vortex traverses an interval  $\Delta l$  is

$$\bar{v}^{-1} \equiv \frac{\Delta t}{\Delta l} = \langle v^{-1} \rangle_a. \quad (3.20)$$

The expectation value is that of the instantaneous inverse velocity with respect to arc length. A detailed calculation of the velocity distribution function shows that although the variable  $v^{-1}$  has some probability of being quite large, the distribution is sufficiently well behaved so that the expected value and variance of  $v^{-1}$  are finite. Thus, the central-limit theorem applies to  $\bar{v}^{-1}$ , which is the average of  $v^{-1}$  over the line segments that make up the perimeter. The result is that the average speed  $\bar{v}$  over many line segments is nearly constant, with fluctuations much smaller than its expected value. Therefore, Eq. (3.19) is expected to be a good approximation for frequencies much below the cutoff, if  $\langle v^{-1} \rangle_a^{-1}$  is used as the velocity.

At this point, it would be straightforward to average the voltage-noise power over an ensemble of noninteracting vortices on orbits of different perimeters  $L$ . To avoid repetition, we defer this process until Sec. IV, where the result is obtained as the zero-drag limit of the corresponding function in the presence of drag.

We would like to emphasize that the vortex percolation mapping described above is quite different from the one previously proposed for inhomogeneous superconductors,<sup>21</sup> in which the issue is whether

the superconducting grains connect to form an infinite conducting path. In this latter case, a series of samples of carefully controlled composition is required to see critical scaling. In contrast, we have described a situation in which the low-frequency response originates near the percolation threshold. The entire range of percolation parameters  $p$  can be investigated in a single sample by making measurements at a variety of frequencies.

It is instructive to contrast the results obtained above with those of an alternative approach. Beginning with Eq. (3.1) and the same model potential, it is evident that a vortex's trajectory is altered radically each time it travels a distance of order  $b$  and enters a new region of the potential. It is reasonable (and incorrect) to assume that after scattering several times off of potential irregularities, the vortex has lost all memory of its initial conditions and diffuses at random about the irregular surface. This picture can be made quantitative by use of a diagrammatic perturbation series, employing a Dyson equation to sum a given class of diagrams (we will not reproduce the details of such a calculation here). This diffusion picture leads to a continuous voltage noise-power spectrum with noise power at zero frequency (implying dc resistivity), in sharp contrast to Eq. (3.19). In reality, a type of classical vortex confinement operates. A vortex, though it initially wanders away from its starting point, will always return and thereafter continue repeating the same closed orbit.

## IV. EFFECT OF DRAG

### A. General discussion

In this section we consider the effect of introducing a small amount of drag into Eq. (2.13) and calculate the thermal average of the resulting noise spectrum. This introduction of drag corresponds to a nonzero parameter  $\Gamma$ , with  $\Gamma \ll \alpha$ . Choosing  $\Gamma$  nonzero automatically introduces Langevin noise, according to Eqs. (2.15) and (2.16). In the zero-drag limit, we find that for small  $\omega$  the voltage-noise power averaged over all trajectory lengths  $L$  obeys

$$P(\omega) \sim \omega^{p_2}, \quad (4.1)$$

with  $p_2 \simeq 0.4$ . In the presence of Langevin noise and drag, we will show that Eq. (4.1) is convolved with a function of unit area and width  $\omega_c$ . For frequencies larger than  $\omega_c$ , Eq. (4.1) is approximately obeyed, while for frequencies smaller than  $\omega_c$ ,  $P(\omega)$  is nearly constant (see Fig. 5). The crossover fre-



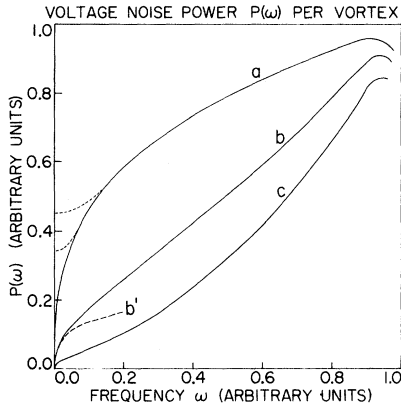


FIG. 5. Solid lines are a plot of the voltage noise power given by Eq. (4.15) for vortices moving without drag. Curve *a* is at temperature  $\beta V = 0.01$ , *b* at  $\beta V = 6.0$ , and *c* at  $\beta V = 10.0$ . At high temperatures (*a*),  $P(\omega) \sim \omega^{p_2}$  up to a high-frequency cutoff. At lower temperatures the noise power deviates from power-law scaling at smaller frequencies; curve *b'* represents pure power-law scaling. The broken lines, shown only on curve *a*, illustrate the modification in the voltage noise-power spectrum at two different levels of drag. The curves should be normalized so that each contains an approximately equal area. (This was not done for clarity of presentation.) The magnitude of the low-frequency noise power, with or without drag, decreases rapidly with decreasing temperature.

quency  $\omega_c$  approaches zero as  $\Gamma$  approaches zero. This is analogous to an ordinary magnetic-phase transition, where the voltage noise power  $P(\omega)$  corresponds to the magnetization  $M$  as follows:

$$P(\omega) \sim \omega^{p_2} \leftrightarrow M(T) \sim (T_c - T)^{\beta'}. \quad (4.2)$$

Adding a small magnetic field  $h$  to the magnetic problem obscures the  $\beta'$  power-law behavior for temperatures approaching the critical temperature, and a new critical exponent appears at  $T_c$

$$M \sim h^{1/\delta}. \quad (4.3)$$

Langevin noise in a thin film plays a role analogous to that of the ordering field in the magnetic problem. It is interesting that Langevin noise has the same effect in the period-doubling bifurcation to chaos sequence of one-dimensional nonlinear maps.<sup>22</sup>

As a preliminary step in deriving the above results for  $P(\omega)$ , consider the situation in which a vortex is on a very long closed fractal of energy  $E_1$ . The Langevin noise  $\vec{\eta}(t)$  is the sum of uncorrelated delta functions. We allow just one of these delta functions to act, and then turn off the drag and

Langevin noise. How does the subsequent motion (path 2, of energy  $E_2$ ) differ from the motion that would have occurred if the delta function had not acted (path 1)? The two paths will begin a distance  $\delta u$  apart, where  $\delta u$  is the component of  $\vec{\eta}(t)$  that is perpendicular to path 1 at time  $t$ . For quite some distance, path 2 will track closely beside path 1, tending on the average neither to get closer nor farther away.<sup>23</sup> Eventually, however, path 1 will run beside a vertex  $j$  of energy between  $E_1$  and  $E_2$ . At this point, path 1 and path 2 will split apart, each following its own constant energy contour to opposite sides of the vertex. If the vertex  $j$  is not a saddle point<sup>24</sup> the paths will immediately rejoin. However, if vertex  $j$  is a saddle point, the paths will dramatically split apart, each going its separate way. The vortex has then changed to a different fractal at vertex  $j$  (see Fig. 4).

With this picture in mind, what is the result if weak drag and Langevin noise are allowed to run continuously? Since the Langevin noise is not deterministic,  $E_2(t)$  is a random variable which is to good approximation Gaussian.<sup>25</sup> At time zero, the vortex is assumed to have energy  $E_1$ . As  $t$  grows, the mean value of  $E_2(t)$  will decrease monotonically and the variance will increase monotonically. After a sufficiently long time  $t$  the vortex will, with high probability, encounter a saddle point of energy between  $E_1$  and  $E_2(t)$ , at which time it will change to a different fractal. Waiting longer, the vortex will eventually change to a third, then fourth fractal, etc. The essential difference from the zero Langevin noise behavior is that the motion is no longer periodic, so that there is now noise power in  $\dot{y}$  at zero frequency. If  $\tau$  is the mean time that a vortex stays on a given fractal, then the motion on time scales much shorter than  $\tau$  is basically unchanged from the drag-free case. For times much greater than  $\tau$ , the motion is quite different (it is diffusive). One expects a crossover from

$$P(\omega) \sim \omega^{p_2} \text{ to } P(\omega) \sim \text{const} \quad (4.4)$$

for  $\omega < \omega_c$ , with  $\omega_c = \tau^{-1}$ .

## B. Quantitative derivation

The following is a quantitative derivation of the crossover behavior obtained above on intuitive grounds. Let  $y(l)$  represent the actual path (parametrized by arc length  $l$ ) taken by a vortex in the presence of weak Langevin noise. It begins with a segment  $s_1$  of a closed fractal of length  $L_1$ , continues with a segment  $s_2$  of a distinct fractal of

length  $L_2$ , etc. The length  $s_j$  may be greater than  $L_j$ , in which case the vortex makes more than one circuit before leaving the closed curve. As before, we require the expectation value  $\langle b_k b_{-k} \rangle$  of the Fourier coefficients to calculate the voltage noise power induced by the vortices. The Fourier coefficient  $b_k$  is defined as

$$b_k \equiv (S_T)^{-1/2} \int_0^{S_T} dl e^{-ikl} y(l), \quad (4.5)$$

where the total arc length  $S_T$  is  $S_T \equiv \sum_{j=1}^N s_j$ . The

$$\langle b_k b_{-k} \rangle = \frac{b'}{2\pi S_T} \sum_{n=1}^N s_n^2 \left[ \frac{L_n}{2\pi} \right]^{p_1-1} \sum_m j_0^2 \left[ \left[ \frac{2\pi m}{L_n} - k \right] \frac{s_n}{2} \right] m^{-p_1} \Theta(|m| - \frac{1}{2}). \quad (4.7)$$

Here  $N$  is the number of distinct fractals in the sum and  $j_0(x) = [\sin(x)]/x$ . The theta function serves merely to exclude the  $m=0$  term from the sum. We approximate the sum on  $m$  in Eq. (4.7) as an integral, with due attention to the excluded region about  $m=0$ . This results in

$$\langle b_k b_{-k} \rangle = b' \int dq q^{-p_1} \left\langle \frac{s}{2\pi} j_0^2[(q-k)s/2] \times \Theta(|q| - \pi/L) \right\rangle_a. \quad (4.8)$$

The expectation subscripted by  $a$  is with respect to arc length

$$\langle w \rangle_a \equiv \left[ \sum_{n=1}^N s_n w_n \right] / \left[ \sum_{n=1}^N s_n \right]. \quad (4.9)$$

Assuming that the arc length  $s$  traveled along a fractal is independent of the length of the fractal  $L$ , the expectation value factors<sup>26</sup> into  $fg$  with

$$f(k) \equiv \left\langle \frac{s}{2\pi} j_0^2(ks/2) \right\rangle_a, \quad (4.10)$$

$$g(k) \equiv \left\langle \Theta \left[ k - \frac{\pi}{L} \right] \right\rangle_a.$$

The function  $f$  is a non-negative even function of unit area. If the distribution function for  $s$  is peaked about  $\langle s \rangle$ , then  $f$  has a width of approximately  $\langle s \rangle^{-1}$ . Generically, one can represent  $f$  as

$$f(q) \simeq \frac{1}{\pi \langle s \rangle} (q^2 + \langle s \rangle^{-2})^{-1}. \quad (4.11)$$

To calculate  $g$ , we make the standard assumption in critical phenomena that the sums over clusters of

corresponding voltage noise power is

$$P(\omega) = \frac{\pi}{2v} \left[ \frac{\hbar}{eL_1} \right]^2 \omega^2 \langle b_{\omega/v} b_{-\omega/v} \rangle. \quad (4.6)$$

In what follows, we will make the assumption that the paths on successive fractals are uncorrelated. We believe this to be an adequate approximation, although it is not strictly correct (there is some correlation remaining since the paths do not intersect each other). Using Eqs. (3.2) and (3.8), straightforward manipulations yield

energy parameter  $\tilde{\epsilon}$  are dominated by clusters of perimeter  $L$  with

$$L = \tilde{c} |\tilde{\epsilon}|^{-1/\sigma}. \quad (4.12)$$

The energy is given by  $E = \tilde{\epsilon}V$ , where  $\tilde{\epsilon}$  is between  $-\frac{1}{2}$  and  $\frac{1}{2}$ . Using the Boltzman factor<sup>27</sup> to give the relative weight of different energy levels, we obtain

$$\langle \Theta(L - \pi/|q|) \rangle_a = \frac{\sinh \left[ \beta V \left[ \frac{\tilde{c}|q|}{\pi} \right]^\sigma \right]}{\sinh(\beta V/2)}. \quad (4.13)$$

Using this result with Eqs. (4.6) and (4.8), we find

$$P(\omega) = \left[ \frac{\hbar}{eL_1} \right]^2 \frac{\pi b'}{2v \sinh(\beta V/2)} \omega^2$$

$$\times \int dq f(q - \omega/v) |q|^{-p_1}$$

$$\times \sinh \left[ \beta V \left[ \frac{\tilde{c}|q|}{\pi} \right]^\sigma \right]. \quad (4.14)$$

Equation (4.14) is the desired relation for the voltage-noise power due to vortices in the presence of drag.

In the zero-drag limit,  $f(q-k) \rightarrow \delta(q-k)$ , and

$$P(\omega) = \left[ \frac{\hbar}{eL_1} \right]^2 \frac{\pi b'v}{2 \sinh(\beta V/2)} \left[ \frac{|\omega|}{v} \right]^{2-p_1}$$

$$\times \sinh \left[ \beta V \left[ \frac{\tilde{c}|\omega|}{\pi v} \right]^\sigma \right]. \quad (4.15)$$

In the limit of no drag and high temperature ( $\beta V \ll 1$ ), we obtain pure power-law scaling out to the order of the high-frequency cutoff  $\omega_{\max} \simeq v/b$  (or the gap frequency, whichever is smaller). Thus the voltage noise power is given by

$$P(\omega) \sim \omega^{p_2}, \quad (4.16)$$

with  $p_2 = \sigma - 2\sigma\nu + 1 \simeq 0.4$ . For  $\beta V \gtrsim 1$ , this power law applies only so long as the argument of the hyperbolic sine in Eq. (4.15) is much less than one (small frequencies). As  $\omega$  increases, the resistance increases more rapidly than a simple power law (see Fig. 5). We note that the exact form of the deviations from power-law scaling found at low temperatures and large frequencies is not universal. The analytic form that the hyperbolic sine assumes for large arguments applies only for the model in which the random variable  $U_j$  describing the potential is uniformly distributed. A different, qualitatively similar result would apply if  $U_j$  were Gaussian, for example. The low-frequency scaling [Eq. (4.16)] however, is universal.

To use Eq. (4.14) in the presence of drag, we require  $f(k)$  as a function of the drag parameter  $\Gamma$ . By Eq. (4.10),  $f$  can be obtained from the distribution function of  $s$ , the arc length a vortex travels before changing fractals. An approximate derivation of this distribution function is sketched in Appendix A.

Using Eqs. (A4) and (3.7), we can obtain the dc resistivity per square as a special case of relation (4.14)

$$R_{sq} = c \left[ \frac{\hbar}{e} \right]^2 \frac{Hvb}{\phi_0 V} \left[ t^2 \sinh \left[ \frac{1}{2t} \right] \right]^{-1} \times (\Gamma t / \alpha)^{(1+\sigma-2\sigma\nu)/3}. \quad (4.17)$$

Equation (4.17) is valid in the low-drag limit. We have assumed that a magnetic field  $H$  has injected a density  $H/\phi_0$  of vortices, where  $\phi_0 = hc/2e$  is the quantum of flux. The vortices are further assumed to move independently; see Sec. V for a discussion of independence. The variable  $t = (\beta V)^{-1}$  is a dimensionless temperature,  $c$  is an undetermined constant of order unity, and the exponent is approximately 0.1.

The ratio of the resistance in the presence of a potential to the resistance for  $V \equiv 0$  is given by

$$\frac{R_{sq}}{R_{sq}^0} = c \frac{\beta V}{2 \sinh(\beta V/2)} (\alpha \beta V / \Gamma)^{(2\sigma\nu+2-\sigma)/3}, \quad (4.18)$$

where  $\alpha$  is of order  $(2\pi\hbar)^{-1}$  [see Eq. (2.14)]. The exponent is approximately 0.9. The hyperbolic sine term causes the resistance to go rapidly to zero at low temperature. This is a consequence of the fact that as  $t \rightarrow 0$ , the vortices are largely confined on small low-energy closed curves and are thus not very mobile. At high temperatures ( $\beta V \ll 1$ ), the inhomogeneities actually increase the resistance over that of a homogeneous sample as the drag  $\Gamma$  goes to zero. This is because the vortices spend time on large fractals and are highly mobile; their velocity, however, approaches zero as the potential strength  $V$  approaches zero.

Once  $\Gamma$  has become so large that either (1) a vortex diffuses a distance  $b$  perpendicular to its ideal (zero-drag) trajectory faster than it travels a distance  $b$  along the trajectory ( $\Gamma/\alpha\beta V > 1$ ), or (2) a vortex is taken by drag in the perpendicular direction faster than along the ideal trajectory ( $\Gamma/\alpha > 1$ ), the function  $f$  becomes as wide as the high-frequency cutoff. At this point no trace remains of the universal power-law behavior. When the amount of drag becomes large, vortex dynamics cease to play an important role, and the motion is that of classical particles diffusing between potential wells.

## V. RELATION TO EXPERIMENT

The most important requirement of the theory is that the vortices be in the low-drag regime (that they drift nearly parallel to the local velocity of the supercurrent). In a material that is not granular, Nozières and Vinen<sup>11</sup> suggest that a superconductor will be in the low-drag regime if the Hall angle for the normal material is nearly  $90^\circ$  in a magnetic field  $H_{c2}$ , or equivalently if  $\omega'_c \tau' \gg 1$ , where  $\omega'_c$  is the cyclotron frequency at  $H_{c2}$  and  $\tau'$  is the scattering time for an electron. This condition appears to be difficult to achieve in films.

We speculate that vortices may move with low drag in granular superconducting films whose correlation length  $\xi_v$  is smaller than the grain size. (This holds approximately in some NbN films,<sup>28</sup> but not in granular aluminum.) An intuitive reason for the low drag is that there are very few conduction electrons available to dissipate energy in a vortex core that resides in the insulating region of a granular superconductor. The low-drag dynamics are experimentally observed in long tunnel junctions (see Appendix D).

It would be useful to experimentally determine the drag parameter  $\Gamma/\alpha$  to check directly whether a

given sample contains vortices moving with low drag. This type of measurement is complicated by inhomogeneities, although a determination of the vortex Hall angle at frequencies greater than the high-frequency cutoff seems promising.<sup>29</sup>

Assuming that a low-drag sample can be found, we now discuss the range of applicability of the theory. There is no particular requirement that the film be exceedingly thin. Thin films have been used recently to achieve a large transverse screening length  $\Lambda$ . Although it is important to have a large screening length so that the Coulomb analogy is preserved up to great distances (as in tests of the Kosterlitz-Thouless-Berezinskii theory), this work depends in no crucial way on the Coulomb picture. The electrostatics mapping used to calculate the potential  $U$  should be accurate so long as the grain size  $b$  is much smaller than  $\Lambda$ . If desired,  $U$  could be calculated by a more complicated functional that does not rely on the Coulomb picture, which was done by Larkin and Ovchinnikov<sup>30</sup> for weak inhomogeneities. This procedure would generate a similar random function  $U$  for a disordered substrate. The notion that vortices drift in the local superflow remains valid independent of the magnitude of  $\Lambda$ .<sup>9</sup> The only limitation on the thickness of the film is that bending modes of the vortex do not play a significant role.

The single-vortex calculations are most likely to be relevant for a sample in which a low density of vortices is injected by an external magnetic field  $H \ll H_{c2}$ , where the vortex density is given by  $n = H/\phi_0$ . We assume that the temperature is not high enough to excite a large number of  $\pm$  pairs. If the mean distance  $d$  between vortices is much greater than  $\Lambda$ , the vortices are essentially independent, and the noise power is given by Eq. (4.14) multiplied by the number of vortices present. As a result, independent vortex dynamics should be more evident in thicker films with reduced  $\Lambda$ .

If the vortices are injected as above with  $\Lambda$  greater than or of the order of  $d$ , they can crystallize into a triangular lattice,<sup>31</sup> which, however, will melt at a finite temperature.<sup>32</sup> The noise power of a vortex lattice is discussed in Appendix C. If the lattice has melted, it is plausible that the situation would be described fairly well by the independent vortex picture, with vortex-vortex interactions lumped into the noise term  $\eta$ . It is possible but not compelling that the above picture would also apply to a neutral plasma where the screening length is sufficiently small so that vortices act independently.

The type of data most suitable for comparison with this theory would come from a low-drag film

containing vortices injected by a magnetic field. The magnetic field should be sufficiently weak so that the noise power is linear in  $H$ , corresponding to independent vortices. The temperature should be somewhat lower than  $T_{2D}$ , so that the density of  $\pm$  pairs is negligible compared with the injected vortex density  $H/\phi_0$ , but not so cold that a vortex lattice forms. Measurements of the voltage noise power or resistivity should be made over a broad range of frequencies.

The regime described above is the natural one for studying the effects of vortex-substrate interactions ("pinning"), both for the present low-drag theory and for other high-drag theories. Pinning effects, which are usually present in films,<sup>33</sup> can be studied directly in this regime. The number of vortices contributing to the resistance is under external control, and the vortex-substrate interactions are not entangled with those due to an unknown number of strongly interacting vortex pairs, as would be the case for  $H = 0$ .

The authors are aware of no systematic frequency-dependent data in the above described regime (see, however, Gittleman and Rosenblum,<sup>29</sup> who have taken frequency-dependent data on a presumably high-drag film at large magnetic fields,  $H = \frac{1}{2}H_{c2}$ ). There are dc data available, which can be compared with the zero-frequency limit of this theory, Eq. (4.17). Gubser and Wolf<sup>28</sup> have measured the temperature-dependent resistance of granular NbN films. The magnetic fields used are apparently not small enough that the resistance is linear in  $H$ . However, we find that the temperature dependence of  $R$  at fixed  $H$  can be fitted quite accurately by the functional form of Eq. (4.17), with the assumption that the only temperature dependence enters explicitly through the factor  $\beta = (k_B T)^{-1}$ . Gubser and Wolf fit a power law to the same data. It is not possible to determine which is the better fit from the data they have published. We note that an accurate fit to Eq. (4.17) should not in itself be taken as a proof that this low-drag theory is correct for NbN. Most of the temperature dependence is provided by the term  $\exp(-V/k_B T)$ , which would also be present in the high-drag limit as vortex diffusion is impeded by the high barriers they must cross. Systematic frequency-dependent data would be needed to distinguish which model applies.

A further, less rigorous comparison with experiment can be made if we make the ansatz that only free vortices contribute to the dc resistance of a film in the absence of a magnetic field. Replacing  $H/\phi_0$  in Eq. (4.17) by the Kosterlitz-Thouless expression<sup>5</sup>  $n_{\text{free}} \sim \exp[-c/(T - T_{2D})^{1/2}]$ , we see that in the

neighborhood of  $T_{2D}$  the resistance is given by  $\text{const} \times n_{\text{free}}$  plus analytic terms. Thus, dc resistance data that is consistent with the Kosterlitz-Thouless vortex theory is consistent as well with the form of Eq. (4.17).

## VI. SUMMARY AND CONCLUSIONS

The equations describing vortex motion in an inhomogeneous film have been rewritten in terms of the energy of a vortex, rather than in terms of the local superflow velocity. This formulation allows a derivation of the voltage noise-power spectrum of a vortex in the absence of drag, based on the fact that a vortex trajectory is periodic. By drawing an analogy to the percolation problem, it is found that the voltage noise power and the resistivity are described at low frequencies by the universal relation  $P(\omega) \sim \omega^{p_2}$ . The exponent  $p_2$  is given in terms of percolation-critical exponents,  $p_2 = \sigma(1 - 2\nu) - 1$ . The introduction of a small amount of drag causes the noise power to deviate from the scaling form at small frequencies. This results in dc resistivity, which cannot be caused by inhomogeneities in the absence of drag.

The resistivity we have calculated is the *linear* response of the system to an applied current. We have not made predictions concerning the nonlinear measurements which are often made.<sup>34</sup>

The case of many vortices interacting without drag on a *homogeneous* substrate was shown to be trivial from the point of view of the voltage noise-power measurements we describe. The corresponding situation on an inhomogeneous substrate was not treated in general, but only in a few specialized regimes.

## ACKNOWLEDGMENTS

It is a pleasure to thank A. Katz for his constant encouragement and advice, D. Browne for a number of helpful insights, M. Beasley for useful conversations and the suggestion that the calculation in Appendix B be performed, and C. Caroli for stimulating discussions and for her hospitality at the Universite de Paris VII, where part of this study was completed. This work was partially supported by the National Science Foundation under Grant No. DMR-80 07934. One of us (S.D.) also acknowledges partial support from CNRS.

## APPENDIX A: DETAILS OF THE NONZERO-DRAG CASE

The energy change of a vortex in the presence of drag is given by  $\tilde{\epsilon}(t) \equiv (E_2(t) - E_1)/V$ , which is ap-

proximately a Gaussian random variable of mean  $\mu(t)$  and variance  $\sigma^2(t)$ . According to Eq. (2.13),  $\mu$  decreases monotonically from zero because of the  $\Gamma$  drag term, while  $\sigma^2$  increases monotonically from zero due to the Langevin noise  $\tilde{\eta}(t)$ . Quantitatively

$$\begin{aligned} \frac{d}{dt}\mu &= \frac{-\Gamma V}{|\psi|^2 d} |\vec{\nabla}u|^2, \\ \frac{d}{dt}\sigma^2 &= 2D |\vec{\nabla}u|^2, \end{aligned} \quad (\text{A1})$$

where  $u = U/V$ . The average size of  $\tilde{\epsilon}(t)$  is

$$\langle \tilde{\epsilon}^2(t) \rangle^{1/2} = [\sigma^2(t) + \mu^2(t)]^{1/2}. \quad (\text{A2})$$

As a vortex travels it passes adjacent to a sequence of saddle-point vertices, each differing in energy from  $E_1$  by an amount  $\Delta U_j$ . After the vortex has traveled  $N$ -lattice spacings, the smallest  $\Delta U_j$  yet encountered will have an average value of the order of  $V/N$ . By equating  $\langle \tilde{\epsilon}^2(t) \rangle^{1/2}$  with  $N^{-1}$ , we obtain a relation for the average number of lattice spacings  $\bar{N}$  that a vortex travels before changing fractals. With the use of Eqs. (A1) and (A2),  $\bar{N}$  is found to satisfy the quartic equation

$$\bar{N}^4 + f'_1 \frac{\alpha k_B T}{\Gamma V} \bar{N}^3 - f'_2 (\alpha/\Gamma)^2 = 0, \quad (\text{A3})$$

where the symbols  $f'$  are positive constants of order unity which depend on the particular model chosen for the potential. In the low-drag limit [ $\Gamma/\alpha \ll (k_B T/V)^2$ ], the appropriate root of Eq. (A3) is

$$\bar{N} = f_1 \left[ \frac{\alpha V}{\Gamma k_B T} \right]^{1/3}. \quad (\text{A4})$$

This is the regime in which  $\sigma^2$  dominates  $\mu^2$  in Eq. (A2). In the opposite limit, the root is

$$\bar{N} = f_2 (\alpha/\Gamma)^{1/2}. \quad (\text{A5})$$

The average arc length is then  $\langle s \rangle = \bar{N}b$ . An approximate calculation (not reproduced here) gives the entire distribution function for  $s$ , which is in fact peaked about  $\langle s \rangle$ . In the low-drag regime

$$\rho(s) \sim s^{1/2} \exp[-(s/\langle s \rangle)^{3/2}]. \quad (\text{A6})$$

This last form allows one to calculate the function  $f(k)$  using Eq. (4.10). As the integral is complicated, one can alternatively use the approximate form (4.11) with  $\langle s \rangle$  given by Eqs. (A4) and (A5).

## APPENDIX B: NOISE POWER IN VOLTS

Equation (4.14) for the voltage noise power of a vortex was derived from scaling arguments, and

characteristically contains an unspecified proportionality constant. Although the constant is nonuniversal and thus depends on the detailed nature of the potential  $U$ , one can obtain an order-of-magnitude estimate for some situations of interest.

The voltage noise power  $P(\omega)$  is defined such that at any given time  $t$

$$\langle V^2(t) \rangle = \int_{-\omega_m}^{\omega_m} d\omega P(\omega), \quad (\text{B1})$$

where  $\omega_m$  is a high-frequency cutoff. The proportionality constant for  $P(\omega)$  is fixed by making an independent estimate of  $\langle V^2(t) \rangle$ . Using Eq. (2.19), the average voltage noise power can be obtained from the average vortex velocity. The velocity, using Eq. (2.13), is given by the energy gradient.

To calculate a typical energy gradient, we assume that variations in thickness and composition lead to a position dependent  $|\psi^2(\vec{r})|d(\vec{r})$ , corresponding to a space-dependent dielectric constant  $\epsilon$ . Let the typical variations in  $\epsilon$  be given by  $\Delta\epsilon = \epsilon_2 - \epsilon_1$ , and the correlation length for  $\epsilon$  be given by  $b$ .

The difference in energy of a charge of radius  $\xi_v$  ( $\xi_v$  smaller than  $b$ ) at two different locations is approximately

$$\Delta U_{\text{Coul}} \simeq \frac{q^2}{2} \ln(b/\xi_v)(\epsilon_2^{-1} - \epsilon_1^{-1}). \quad (\text{B2})$$

To obtain (B2), we have assumed that the bulk of the energy difference is given by the difference of electric field energies in circles of radius  $b$  about the charges. Using a typical energy gradient of  $\Delta U_{\text{Coul}}/b$ , Eq. (2.13) results in the following formula for the average vortex velocity:

$$\langle \vec{v}^2 \rangle^{1/2} \simeq \frac{\hbar}{2mb} \ln(b/\xi_v) \frac{\Delta\epsilon}{\epsilon}, \quad (\text{B3})$$

where  $\Delta\epsilon/\epsilon$  is the typical fractional variation in  $|\psi^2|d$ . This results in the total voltage noise power for a single vortex integrated over all frequencies of

$$\langle V^2(t) \rangle \simeq \frac{1}{2} \left[ \frac{\pi \hbar^2}{2embL_1} \ln(b/\xi_v)(\Delta\epsilon/\epsilon) \right]^2. \quad (\text{B4})$$

For the values  $b = 200 \text{ \AA}$ ,  $\xi_v = 50 \text{ \AA}$ ,  $\Delta\epsilon/\epsilon = 0.2$ , and  $L_1 = 0.1 \text{ mm}$ , this yields an rms voltage of  $\langle V^2(t) \rangle^{1/2} \simeq 10^{-8} \text{ V}$  per vortex, which is the total area under the  $P(\omega)$  curve up to  $\omega_m$ , where  $\omega_m \simeq 2\pi \langle \vec{v}^2 \rangle^{1/2}/b \simeq 10^{11}/\text{s}$  for the parameters given above.

### APPENDIX C: VORTEX LATTICE AND FINITE GEOMETRY EFFECTS

In this appendix we discuss the situation in which the vortices injected by an external magnetic field are at a sufficiently low temperature that a lattice has formed. Several authors, including Schmid and Hauger<sup>35</sup> and Fisher<sup>36</sup> have considered this situation in the large-drag regime in the presence of an inhomogeneous substrate. Tkachenko<sup>37</sup> and Fetter and Hohenberg<sup>38</sup> have done calculations on a vortex lattice in the no-drag regime, but with a uniform substrate.

What is the behavior of a lattice with ideal vortex dynamics in the presence of substrate inhomogeneities? Let  $d'$  be the lattice constant for the vortex lattice, and  $b$  be the correlation length for the potential ( $b$  is the grain size), with  $d' \gg b$ . If the fractional variation in  $\psi^2 d$  is of the order of unity, a vortex will be moving under the influence of image charges of magnitude the order of  $q$ , and a distance of only  $b$  away (see Appendix B). The effect of the local images will overwhelm that of the real vortices, which are a much greater distance  $d'$  away (quantitatively,  $|\vec{\nabla}U| \gg q/d'$ ). We have thus argued that the vortex lattice does not much modify the independent vortex picture. This argument breaks down if the vortex of interest happens to have nearly the median energy, which would potentially put it on a very large orbit. To see this, we observe that a vortex travels on a constant energy contour of the potential

$$U_{\text{total}} = U + \tilde{U}, \quad (\text{C1})$$

where  $\tilde{U}$  is the potential energy due to the rest of the vortex lattice and to the "background charge" caused by the diamagnetic current induced by the external magnetic field. We use the percolation analogy of Sec. III in which vortices circle connected clusters of vertices. The main modification is that the probability  $p(\vec{r})$  that a vertex is occupied and thus available to be part of a connected cluster becomes position dependent for nonconstant  $\tilde{U}$ .

To form a large connected cluster of diameter  $R$ ,  $p$  must be sufficiently close to  $p_c$  (given by  $R \sim |p - p_c|^{-\nu}$ ), and  $p(\vec{r})$  must remain sufficiently close to  $p_c$  at all points on the cluster. There is a maximum size  $R_m$  for which this condition can be satisfied. An approximate calculation, which neglects the time dependence of  $\tilde{U}$  and uses the methods of Appendix B results in

$$R_m/b \simeq c \left[ \ln(b/\xi_v) \frac{\Delta\epsilon d'^2}{eb^2} \right]^{\nu/(2\nu+1)}, \quad (\text{C2})$$

where  $\Delta\epsilon/\epsilon$  is the fractional variation in  $\psi^2 d$ ,  $c$  is a dimensionless constant of order unity, and the exponent is approximately 0.4. Since all clusters larger than  $R_m$  are strongly suppressed, we expect there to be reduced voltage noise power at frequencies smaller than the inverse time  $T^{-1}$  to circumnavigate a cluster of size  $R_m$ . The noise power at higher frequencies should, however, be little affected by the vortex lattice. Equation (C2) implies that a larger part of the scaling region around zero frequency will be obscured the denser the vortex lattice.

A similar cutoff at  $R_m$  should also occur for a single vortex in a finite geometry, where here  $\tilde{U}$  would be due to image vortices. dc resistivity due to finite-size effects could appear in a dissipationless sample if one allows for vortex annihilation and creation in the vicinity of a boundary.

#### APPENDIX D: POSSIBILITIES OF VORTICES IN GRANULAR SUPERCONDUCTING FILMS MOVING WITH LOW DRAG

A granular superconducting film is composed of islands of superconductor separated by channels of insulating material. We suggest that vortex cores residing in the insulating channels may move with very low drag. This contrasts with the high-drag behavior observed in ordinary (nongranular) type-II superconductors.

The insulating channels in granular superconductors are complicated in that the channels branch on the scale of the grain size. It is difficult to deal directly with such a complicated topology, so we will consider instead a vortex core residing in a linear unbranched insulating channel. This is simply a long  $S$ - $I$ - $S$  (superconductor-insulator-superconductor) Josephson junction.

It has been shown experimentally that a vortex in an  $S$ - $I$ - $S$  long junction will be accelerated to enormous velocities by an applied current that is a small fraction of the critical current.<sup>39,40</sup> In particular, Fulton and Dynes<sup>40</sup> have found vortex velocities of  $1.1 \times 10^9$  cm/s in Sn-SnO-Sn tunnel junctions. This striking low-drag behavior was anticipated by the theoretical work of Lebowl and Stephen,<sup>41</sup> who noted that low shunt conductivity (found in  $S$ - $I$ - $S$  junctions) results in weak damping in contrast to the strongly damped vortex motion seen in homogeneous type-II superconductors.

In the remainder of this Appendix we derive an estimate of the drag parameter that would be required if the vortex equations of motion given in Sec. II are to be consistent with experiments on tun-

nel junctions. We note that the theory of Lebowl and Stephen is a more accurate description of vortices in Josephson junctions; our Eq. (2.13) is treated as a phenomenological description of vortex motion that contains adjustable parameters. The Ginzburg-Landau theory is used to describe a long Josephson junction that extends in the  $\hat{x}$  direction. The order parameter  $|\psi^2(\vec{r})|$  is assumed to be strongly depressed in the region  $-l/2 \leq y \leq l/2$ , where  $l$  corresponds roughly to the thickness of the insulating layer. The depressed order parameter results in a vortex energy that has a sharp minimum at  $y=0$ . The film is assumed to have a uniform thickness  $d$  in the  $\hat{z}$  direction.

We use Eqs. (2.13) and (2.14), and neglect the part of the drag force that depends on the vortex sign ( $b_2 \equiv 0$ ). For a (+) vortex, the velocity is given by

$$\vec{v} = \frac{1}{2\pi\hbar |\psi|^2 d (1 + \xi^2)} (-\hat{z} \times \vec{\nabla} U - \xi \vec{\nabla} U), \quad (D1)$$

where  $\xi \equiv b_1/(2\pi\hbar)$ .  $\xi$  is the dimensionless drag parameter,  $\xi = \Gamma/\alpha$ . In steady state, the vortex will have a velocity in the  $\hat{x}$  direction,  $\vec{v} = v\hat{x}$ . Using  $\vec{v} \cdot \hat{y} = 0$ , Eq. (D1) implies

$$v = - \frac{1}{2\pi\hbar\xi |\psi|^2 d} \frac{\partial U}{\partial x}. \quad (D2)$$

The  $x$  component of the energy gradient is proportional to the applied current

$$\frac{\partial U}{\partial x} = \frac{2\pi\hbar}{2e} J, \quad (D3)$$

where  $J$  is the current applied per unit length. Thus, the steady-state vortex velocity as a function of applied current is given by

$$v = \frac{J}{2e\xi |\psi|^2 d}. \quad (D4)$$

It is convenient to substitute for  $|\psi|^2 d$  in terms of the critical current per unit length of the junction

$$J_c = \frac{\hbar e |\psi|^2 d}{ml}. \quad (D5)$$

Equations (D4) and (D5) result in

$$v = \left[ \frac{\hbar}{2ml\xi} \right] \left[ \frac{J}{J_c} \right]. \quad (D6)$$

Using  $l \approx 20 \text{ \AA}$  and the data of Fulton and Dynes, the dimensionless drag parameter  $\xi$  is found to be quite small

$$\xi \approx 10^{-4}. \quad (D7)$$

We have shown that if Eq. (2.13) is applied to long  $S$ - $I$ - $S$  Josephson junctions, it must be used with a very small drag parameter to be consistent with experiment. The small drag parameter should

describe granular superconductors as well if the branched structure does not invalidate the result found for long junctions.

\*Present address: Laboratory of Atomic and Solid State Physics, Clark Hall, Cornell University, Ithaca, New York 14853.

†Present address: Department of Physics and Applied Physics, Stanford University, Stanford, California 94305.

<sup>1</sup>V. L. Berezinskii, Zh. Eksp. Teor. Fiz. **61**, 1144 (1971) [Sov. Phys.—JETP **34**, 610 (1972)].

<sup>2</sup>J. M. Kosterlitz and D. J. Thouless, J. Phys. C **6**, 1181 (1973).

<sup>3</sup>M. R. Beasley, J. E. Mooij, and T. P. Orlando, Phys. Rev. Lett. **42**, 1165 (1979).

<sup>4</sup>S. Doniach and B. A. Huberman, Phys. Rev. Lett. **42**, 1169 (1979).

<sup>5</sup>B. I. Halperin and D. R. Nelson, J. Low Temp. Phys. **36**, 599 (1979).

<sup>6</sup>L. A. Turkevich, J. Phys. C **12**, L385 (1979).

<sup>7</sup>A. Sommerfeld, *Mechanics of Deformable Bodies* (Academic, New York, 1950).

<sup>8</sup>P. G. DeGennes and J. Matricon, Rev. Mod. Phys. **36**, 45 (1964).

<sup>9</sup>A. L. Fetter, P. C. Hohenberg, and P. Pincus, Phys. Rev. **147**, 140 (1966).

<sup>10</sup>J. Bardeen and M. J. Stephen, Phys. Rev. **140**, A1197 (1965).

<sup>11</sup>P. Nozières and W. F. Vinen, Philos. Mag. **14**, 667 (1966).

<sup>12</sup>D. J. Bishop and J. D. Reppy, Phys. Rev. Lett. **40**, 1727 (1978).

<sup>13</sup>V. Ambegaokar, B. I. Halperin, D. Nelson, and E. D. Siggia, Phys. Rev. B **21**, 1806 (1980).

<sup>14</sup>(a) Other relationships between two-dimensional fluids and charges are well known; see, for example, Refs. 13 and 7; (b) W. F. Vinen, Prog. Low Temp Phys. **3**, 1 (1961).

<sup>15</sup>P. W. Anderson, Rev. Mod. Phys. **38**, 298 (1966).

<sup>16</sup>It is the median energy because the percolation threshold is exactly  $\frac{1}{2}$  for site percolation on a triangular lattice.

<sup>17</sup>B. B. Mandelbrot, *Fractals* (Freeman, San Francisco, 1977).

<sup>18</sup>C. Domb, J. Phys. C **7**, 2677 (1974).

<sup>19</sup>D. Stauffer, Phys. Rep. **54**, 1 (1979).

<sup>20</sup>H. E. Stanley, J. Phys. A **10**, L211 (1977).

<sup>21</sup>G. Deutcher and M. Rappaport, J. Phys. C **39**, 581 (1978).

<sup>22</sup>J. P. Crutchfield, J. D. Farmer, and B. A. Huberman, Phys. Rep. (in press).

<sup>23</sup>In the language of ergodic theory, the Lyapunov exponent that describes this regime is zero.

<sup>24</sup>A vertex  $j$  is a saddle point if  $(E_j - E_k)$  changes sign at least 4 times as  $k$  makes a complete cycle through the

six nearest neighbors of vertex  $j$ . A simple calculation shows that at the median energy, half of all vertices are saddle points.

<sup>25</sup>The Gaussian approximation breaks down by the time that  $E_2$  has a substantial probability of being in the neighborhood of at least one of the potential cutoffs at  $\pm V/2$ .

<sup>26</sup>The approximation is quite good for  $s \ll L$ , which is the regime where accuracy is required to obtain the low-frequency power spectrum. The lack of independence for  $s \gg L$  is such that  $P(\omega) \sim \omega^{p_2}$  is obeyed somewhat more accurately than suggested by Eq. (4.14) for  $\omega > \omega_c$ .

<sup>27</sup>According to Eq. (2.17), the dielectric constant  $\epsilon$  enters into the probability function. We approximate, using the average  $\langle \epsilon \rangle$  on trajectories of zero energy. Variations of  $\langle \epsilon \rangle$  on trajectories of different energy will cause deviations from perfect scaling at large frequencies, in addition to that explicitly exhibited in Eq. (4.15). Similar deviations result as Eqs. (3.14) and (3.15) become inaccurate for  $|p - p_c|$  large.

<sup>28</sup>D. U. Gubser and S. A. Wolf, in *Ordering in Two Dimensions*, edited by S. K. Sinha (North-Holland, New York, 1980), p. 471.

<sup>29</sup>J. I. Gittleman and B. Rosenblum, Phys. Rev. Lett. **16**, 734 (1966).

<sup>30</sup>A. I. Larkin and Y. N. Ovchinnikov, Zh. Eksp. Teor. Fiz. **61**, 1221 (1971) [Sov. Phys.—JETP **34**, 651 (1972)].

<sup>31</sup>A. A. Abrikosov, Zh. Eksp. Teor. Fiz. **32**, 1442 (1957) [Sov. Phys.—JETP **5**, 1174 (1957)].

<sup>32</sup>B. A. Huberman and S. Doniach, Phys. Rev. Lett. **43**, 950 (1979).

<sup>33</sup>See, for example, A. F. Hebard and A. T. Fiory, in *Ordering in Two Dimensions*, edited by S. K. Sinha (North-Holland, New York, 1980), p. 181.

<sup>34</sup>See, for example, R. F. Voss, C. M. Knoedler, and P. M. Horn, Phys. Rev. Lett. **45**, 1523 (1980).

<sup>35</sup>A. Schmid and W. Hauger, J. Low Temp. Phys. **11**, 667 (1973).

<sup>36</sup>D. S. Fisher, Phys. Rev. B **22**, 1190 (1980).

<sup>37</sup>V. K. Tkachenko, Zh. Eksp. Teor. Fiz. **50**, 1573 (1966) [Sov. Phys.—JETP **23**, 1049 (1966)].

<sup>38</sup>A. L. Fetter and P. C. Hohenberg, Phys. Rev. **159**, 330 (1967).

<sup>39</sup>J. T. Chen, T. F. Finnegan, and D. N. Langenberg, Physica (Utrecht) **55**, 413 (1971).

<sup>40</sup>T. A. Fulton and R. C. Dynes, Solid State Commun. **12**, 57 (1973).

<sup>41</sup>P. Leubwohl and M. J. Stephen, Phys. Rev. **163**, 376 (1967).